

# Nanostructure analysis using spatially modulated illumination microscopy

David Baddeley<sup>1</sup>, Claudia Batram<sup>1</sup>, Yanina Weiland<sup>1</sup>, Christoph Cremer<sup>1–3</sup> & Udo J Birk<sup>1,4,5</sup>

<sup>1</sup>Kirchhoff Institut für Physik, Universität Heidelberg, INF 227, D-69120 Heidelberg, Germany. <sup>2</sup>Institute for Pharmacy and Molecular Biotechnology, Universität Heidelberg, D-69120 Heidelberg, Germany. <sup>3</sup>Institute of Molecular Biophysics, The Jackson Laboratory, Bar Harbor, Maine 04609, USA. <sup>4</sup>King's College London, Randall Division of Cell & Molecular Biophysics, London SE1 1UL, UK. <sup>5</sup>Institute of Electronic Structure & Laser—FORTH, PO Box 1527, Vassilika Vouton, 71110 Heraklion, Greece. The authors' lab group: Applied Optics and Information Processing, University of Heidelberg ([http://www.kip.uni-heidelberg.de/AG\\_Cremer/](http://www.kip.uni-heidelberg.de/AG_Cremer/)). Correspondence should be addressed to D.B. ([baddeley@kip.uni-heidelberg.de](mailto:baddeley@kip.uni-heidelberg.de)).

Published online 18 October 2007; doi:10.1038/nprot.2007.399

**We describe the usage of the spatially modulated illumination (SMI) microscope to estimate the sizes (and/or positions) of fluorescently labeled cellular nanostructures, including a brief introduction to the instrument and its handling. The principle setup of the SMI microscope will be introduced to explain the measures necessary for a successful nanostructure analysis, before the steps for sample preparation, data acquisition and evaluation are given. The protocol starts with cells already attached to the cover glass. The protocol and duration outlined here are typical for fixed specimens; however, considerably faster data acquisition and *in vivo* measurements are possible.**

## INTRODUCTION

SMI microscopy is a form of structured illumination microscopy. Unlike other forms of structured illumination, it does not deliver an increase in the imaging resolution, but allows instead high-precision measurements of object size and position. This protocol can potentially be applied to extract structural parameters of a variety of macromolecular compounds, for example, those engaged in replication and transcription<sup>1</sup>, to specific gene regions<sup>2</sup>, to membrane-bound complexes and to many other biomolecular machines. It is particularly suitable to studies at the single-cell level. Application to tissue sections, although possible, poses an additional set of difficulties (mostly owing to lack of optical sectioning) and is not discussed here. Alternative methods to obtain similar structural information are electron microscopy as well as novel high-resolution light microscopy techniques, such as STimulated Emission Depletion (STED)<sup>3</sup>, Photo-Activated Localisation Microscopy (PALM)<sup>4–6</sup> and nonlinear structured illumination<sup>7,8</sup>.

The structured illumination in the SMI microscope takes the form of a standing wave along the optical axis, created through the interference between two counter-propagating laser beams. This structured illumination renders information accessible that would be lost in conventional microscopes owing to the blurring of the object by the microscope's optics.

## Experimental design

The layout of the SMI microscope is shown in **Figure 1**. The laser light is split into two beams of equal intensities by a 50:50 beam splitter such that it illuminates the sample from both sides via two objective lenses aligned on the same optical axis (*z* axis). Interference of the laser light results in a standing wave and thus a highly structured illumination along the *z* axis. Samples are prepared using standard object slides and standard coverslips. Using a piezo stage, the object is moved along the *z* axis and a 2D image is recorded at every *z* position resulting in a 3D data stack of the fluorescence intensities. Only the right-hand objective lens (OL1 in **Fig. 1a**), imaging through the coverslip, is used to collect the fluorescence detected by a highly sensitive black-and-white charge-coupled device (CCD) camera. Fluorophores in the sample get

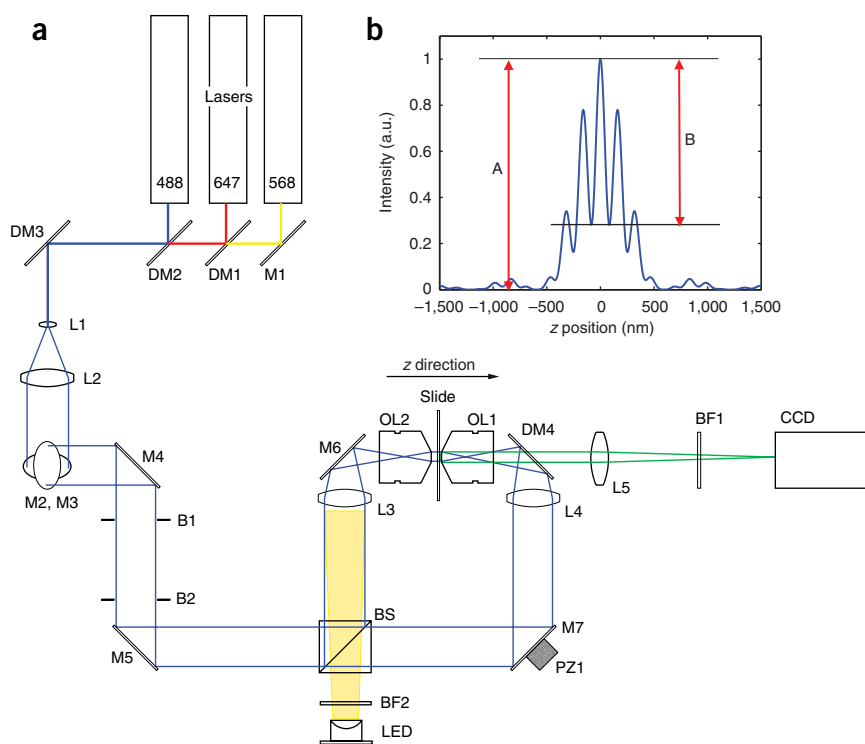
excited according to the illumination intensity at a given *z* position, resulting in a modulation of the detected fluorescence light (**Fig. 1b**).

From this signal, further structural information (e.g., size<sup>9</sup>, position<sup>10</sup>, shape<sup>11</sup>) about the object may be obtained. However, as the optical resolution itself is not increased, prior information, usually in the form of assumptions about the object, is necessary to extract this information. When performing size estimation, a spherical fluorophore distribution within the fluorescently labeled object is usually assumed. The modulation depth (the ratio *B/A* in **Fig. 1b**) is extracted from an axial profile through the object of interest and compared to a theoretical model for objects of the assumed shape (obtained by analytically or numerically convolving a functional description of the object with the simplified functional description of the PSF).

For spherical objects, size measurements are possible with a precision of around 5 nm over a size range of around 40–200 nm. The behavior for nonspherical objects can be analyzed by computer simulation (our unpublished data). For nonspherical but relatively compact objects (i.e., objects without holes or other significant substructure), a good scaling relationship is maintained over a size range of around 40–160 nm. Owing to the imperfect agreement with the spherical model and the difficulty of defining a diameter for an arbitrary object form, the estimated sizes can no longer be regarded as the exact size (a bias of  $\pm 30$  nm is quite possible). This does not present a problem for relative measurements, but should be considered when a comparison to other measurement techniques such as electron microscopy is made. The interpretation of the data can, however, become difficult for larger objects that are either sparse or that have significant substructure on a length scale corresponding to the standard size measurement range. In this case, the measured modulation depth is a function of the substructure size and the distances between the various substructure components.

For object position measurements, similar assumptions are required. As the positions are extracted from the position and not the depth of the peaks of the modulation seen in the fluorescence signal (**Fig. 1b**), calibration of the modulation

**Figure 1** | SMI setup. (a) SMI setup using two objective lenses (OL1 and OL2) for illumination, resulting in a standing wave in the object space between the two lenses. The components are as follows: M1–7, mirrors; DM1–4, dichroic beamsplitters; L1 and L2, beam expander; BS, beam splitter; BF1 and BF2, blocking filters; L5, tube lens; L3 and L4, relay lenses; B1 and B2, field diaphragm; PZ1, phase piezo; LED, white LED for transmitted light; CCD, CCD camera. An additional piezo (not shown) controls the movement of the slide along the optical axis. When a small object is moved along the z axis through the focus of the detection objective lens (OL1), an intensity profile (b) is obtained. The modulation depth is then given as the ratio  $r = B/A$ .



contrast is not necessary. However, for distances between objects with different fluorescent labels, the peaks in the different color channels need to be related, for which multispectrally labeled objects are required. Distance measurements with a precision better than 2 nm along the optical axis are routinely possible.

One should note that the experimental layout above is not the only solution; a triangular interferometer setup as used in the 4Pi microscope is also possible. Indeed, similar size measurements have also been carried out with the 4Pi (ref. 12). Our use of a rectangular setup is motivated, in part, by the fact that dichroic filters for 45° incidence are easier to obtain than for other angles.

The dichroic mirror (DM4) and the blocking filter (BF1) block only the laser lines, allowing multicolor acquisitions to be performed in a sequential fashion by operating shutters in front of the lasers. Switching is done automatically by the acquisition software with three (the default number, although the number of channels can be altered in the software) images being obtained at each z position. If cross talk is significant, band-pass filters can be manually switched in place of BF1 using a filter wheel. This, however, necessitates manual sequential acquisition. Changing the dichroic mirror DM4, however, requires a complete realignment of the interferometer (see also **Supplementary Manual** online).

**Overview of the procedure**

Generally, in addition to the actual measurements on the biological sample, a calibration measurement is necessary: (i) for size measurements, to calibrate the modulation of the structured illumination and (ii) for distance measurements, to calibrate the wavefronts of the standing wavefield. For distance measurements, these wavefronts can be thought of as a ‘ruler’ through which the distances are determined. The preparation of both biological

sample and calibration samples are described below. Fluorescent nanospheres (beads) are used as calibration objects.

The SMI microscope is controlled by a software program, the use of which is similar to the software for modern confocal/widefield systems. The most noticeable difference is the absence of an ocular, all focusing and searching being performed using the CCD camera.

The purpose of calibration in size measurements is to determine the depth of the modulation in the illumination pattern. This modulation is typically not complete owing to a small amount of vibrational broadening and slight differences in the intensity of the illumination between the two sides. When uncorrected, this error would result in a systematic overestimation of object sizes.

Although the portion of the illumination pattern that is not modulated is typically small (<5% of the maximum intensity), good measurements are possible with an unmodulated component as high as 30% when this is corrected. In contrast to focused techniques such as 4Pi, the illumination pattern is not hugely affected by the sample refractive index mismatch. Air bubbles and highly absorbing or scattering samples are problematic, but, otherwise, the effect is much less than would be expected. This can be explained by the fact that the illumination uses an effective numerical aperture of 0. The non-focused nature of the illumination also leads to quite a large tolerance (some micrometers) in the positioning of the lenses when compared with focused techniques.

**MATERIALS**

**REAGENTS**

- Fluorescent nanospheres, beads (G100, Duke Scientific or TetraSpeck beads; Molecular Probes), for calibration
- Sample of interest
- Standard BK7 glass coverslip (no. 1.5, 170 μm thickness)

**EQUIPMENT**

- Argon and krypton ion lasers (Ar+ type 95-4, Kr+ type 95-K, Kr+ type 95L-K; Lexel) **! CAUTION** Class IV laser. Wear laser protection goggles during operation.
- Beam combiner (type F33-488; AHF Analysetechnik)



## PROTOCOL

- Beam expander (self-made using a microbank cage and lenses from Linos)
- Beam splitter (NT47-012; Edmund Optics)
- Microscope optics (tube lens and  $\times 100$  oil immersion, NA 1.4 objective lens; Leica Microsystems) for wide field imaging of the fluorescence signal
- 2nd  $\times 100$  oil immersion (NA 1.4 objective lens; Leica Microsystems) used as condenser
- Multi-axis lens holder (type M-461; Newport)
- Multi-axis object-holder positioner (self-made to minimize thermally induced shifts<sup>13</sup>)
- Step motor (ZSS 422-200-1.2; Phytron GmbH)
- Motor driver (mc compact, ITK Dr. F. Kassen)
- Piezo electrical translation stages (type P-731.20; Physik Instrumente GmbH)
- Piezo driver (type E-509.C2, including amplifiers type E-505.00; Physik Instrumente)
- Focusing lenses (type 322266; Linos Photonics)
- Multi-axis focusing lens positioners (type M-LP-05-XYZ; Newport)
- Dichroic filter (type F63-488; AHF Analysetechnik)
- Laser blocking filter (F62-568; AHF Analysetechnik)
- Black/white CCD camera (Sensicam QE; PCO)
- Computers
- Microscope control software (written in Python and C++); it can be obtained by contacting the authors (licensing terms negotiable). The microscope control software is similar to most commercial offerings
- Scientific software (written in Matlab, Mathworks) for developing the data display and analysis routines. The data analysis package for Matlab can be obtained by contacting the authors (licensing terms negotiable). A short description of the analysis package is included in the **Supplementary Manual** online

### EQUIPMENT SETUP

**Optical setup** For details regarding alignment of the optical setup, see the **Supplementary Manual** online.

## PROCEDURE

### General slide preparation for SMI microscopy

- 1| Fix samples on a standard BK7 glass coverslip (no. 1.5, 170  $\mu\text{m}$  thickness). (Although samples may also be prepared on the slide when unavoidable, it is not recommended—preparation on the slide does not affect the interference pattern; it does, however, as for any other light microscope, result in a decrease in the effective imaging resolution and in the observed signal strength). For *in vivo* experiments, a micro-perfusion chamber using coverslips on both sides is available.
- 2| Label according to standard biological protocols (e.g., antibody staining, fluorescence *in situ* hybridization). Alternatively, use *in vivo* labeling through expression of GFP, mRFP or the like. The usable dyes depend on the combination of laser lines and detection filters used. Laser lines for excitation at 458, 488, 514, 568 and 647 nm are available. With the filter sets of our current prototype, dyes with spectra analogous to FITC, TRITC and Cy5 can be used (see **Fig. 1a**).
- 3| If desired (this is recommended), prepare calibration beads on the slide (see **Box 1**). When wishing to perform high-precision distance measurements using multiple spectral signatures, it is essential that multispectral beads are prepared with the sample for calibration. Another possibility is a built-in control object in the form of a biological double labeling. Size measurements are not as critical, allowing the calibration beads to be on a separate slide.
- 4| Invert the coverslip onto a standard microscope slide using a glycerol-based embedding medium containing an antifade agent such as VectaShield and seal with nail polish. Other embedding media, for example, Moviol, are possible; however, media that polymerize, form crystals or have a refractive index too far away from that of glass are a potential source of problems. A series of bead measurements is advisable when contemplating a different embedding. It is also theoretically possible to use substances other than nail polish to attach the coverslip, such as dental silicone (e.g., TwinSil). Substances that are sticky or become sticky in contact with immersion oil (e.g., Fixogum rubber cement) should be avoided, as these may become attached to the objective front lens while inserting or removing the sample.

### SMI image acquisition

- 5| Turn lasers and electronics on, and start the SMI software. Wait for approximately 1 h to allow lasers to warm up and attain stability. This warm-up time is principally a requirement of the gas lasers, which show mode jumps and instability in the

## BOX 1 | PREPARATION OF CALIBRATION SAMPLE

1. Dilute a stock solution of 100 nm fluorescent beads of the same color (i.e., same fluorescence spectra) as the object of interest in the biological sample. For multi-color measurements, use multispectral beads such as TetraSpeck beads (Molecular Probes). In principle, any beads with a size in the range of approximately 40–180 nm could be used, although 40 nm beads are typically rather weak and the larger beads will not allow the same calibration accuracy. In practice, any bead size in the range of 70–140 nm should be usable. The required dilution depends on the bead type, manufacturer and personal experimental style. The aim is to obtain approximately 100–500 well-separated (not clustered) beads within a  $50 \mu\text{m} \times 50 \mu\text{m}$  field of view. For Duke Scientific 100 nm green beads, a dilution of 1:500 is reasonable. A volume of 50–100  $\mu\text{l}$  of diluted solution is more than sufficient. It is recommended that you dilute with ethanol instead of water, as this leads to a more uniform distribution and decreases the drying time.
2. Mix diluted beads thoroughly and place in ultrasound bath for approximately 3 min to break up any clusters.
3. Pipette 10–20  $\mu\text{l}$  of diluted bead solution onto the coverslip/slide and spread with a second coverslip.
4. Leave to dry ( $\sim 5$  min with ethanol dilution and  $\sim 15$  min with distilled water).
5. Embed as per biological specimen.

An alternative is to pretreat the coverslip/slide with poly-L-lysine and potentially use carboxyl modified beads. This is helpful when combined with a biological sample, as some beads may otherwise detach from the slide surface.

output intensity as the cavity warms up and expands. A similar setup using solid-state lasers would have a much shorter warm-up time.

**! CAUTION** During the start-up of the SMI control software, the stepper motor stage will be initialized by moving from end to end. Remove the object holder to avoid damage to the objective lenses and/or misalignment of the system.

#### Initial calibration measurements

6| Thoroughly clean both sides of the sample.

7| Insert slide with calibration beads into the slide holder and move between the two objectives using the joystick control. Once the sample is in position, decrease stepper motor speed to 1.

**! CAUTION** Eye safety risk. Ensure that laser shutters are closed during this procedure.

8| Apply immersion oil to both sides of the sample, allowing a drop to run down and fill the space between the sample and front lens of the objectives. Note that immersion oil cannot be applied before the slide is inserted between the objectives, as it would run down under the influence of gravity.

9| Open the laser shutter and focus using the joystick while observing the fluorescence image on the computer screen.

**! CAUTION** Travel range in between the objective lenses is limited. Touching the objective lenses with the sample might result in a misalignment of the system.

#### ? TROUBLESHOOTING

10| Wait for 3–5 min for the immersion oil to come to rest.

11| Acquire an image stack using an axial step size of 40 nm. Typically 100 slices centered on the focal slice are taken. Save acquired 3D data stack.

12| Repeat Step 11 at 2–3 different lateral locations on the slide.

13| If desired, perform initial data analysis now, to ensure the device is functioning correctly.

#### Measurements of interest

14| Insert biological specimen, as described in Steps 6–10. In addition to fluorescence, transmitted light may be used to find the focal plane/cells of interest. The transmitted light illumination used on the SMI achieves a much better contrast for phase objects than is obtained using visual inspection on a conventional microscope. The reason for this is a combination of a very low effective illumination NA and the use of a high dynamic range CCD camera for detection, allowing the automatic subtraction of the constant high background corresponding to the undiffracted zero order.

15| Find interesting cells and acquire images. An axial ( $z$ ) step size of 40 nm should be used, and the  $z$  range can be set via start and end points as with standard microscope software. (To be correctly sampled, the step size should be less than around 60 nm. As the step size is reduced, the contribution of camera readout noise for the same total photon number increases. A step size of 40 nm is a good compromise, allowing slight oversampling without a noticeable decrease in signal to noise.) The integration time should be set to make the best possible use of the 12-bit dynamic range of the camera. Ideally, the brightest pixel in the in-focus slice should have between 1,000 and 3,000 counts (allowing a little headroom in case one is not in the in-focus slice, after all). When, however, either speed or photobleaching is important, a much lower integration time can be used; good measurements can be made as soon as the signal is approximately 100 counts higher than the background (as long as the background is reasonably low), and it is possible to work with as little as 30 counts.

#### ? TROUBLESHOOTING

16| If performing precision distance measurements, acquire an image of the beads above/below the cell immediately after the measurement of each cell itself. The  $x$ – $y$  position of the sample should not be changed.

17| Repeat Steps 15 and 16 until sufficient cells have been viewed.

#### Final calibration measurements

18| Reinsert calibration slide and take further 3–4 acquisitions to verify that no significant drift/misalignment has occurred during the course of the experiment.

19| Shut down the instrument and turn off lasers.

20| Wait for 10–15 min and then turn off laser cooling.

## Data analysis: calibration

- 21|** The purpose of the calibration measurements is to determine what the modulation depth would be for an infinitely small object. Open bead measurement in SMI analysis software. Select the desired color channel.
- 22|** Enter nominal size of calibration beads in the *bead\_size* parameter field. Set the wavelength parameter ( $med\_k\_eff = (2\pi n/\lambda) \cdot STEPSIZE$ ) to the appropriate value for the refractive index ( $n$ ) and wavelength ( $\lambda$ ) used, the correction value *umod* to zero and all other parameters to the values you intend to use for the biological measurements (standard parameters:  $ROI = 3 \times 3$  or  $5 \times 5$  and *background* =  $9 \times 9$  or  $11 \times 11$ ).
- 23|** Run object identification routine *ofind* and check whether all beads have been identified. If necessary, change parameters for automated object finding (*ofind\_thresh* and *ofind\_blur*) and rerun if necessary.
- 24|** Run fitting routine, *dofits*. A fit is performed on an axial profile extracted at the location of each of the objects found using *ofind*. The function that is fitted is a theoretical description of the axial profile, with the modulation depth and fringe position as two of the parameters. A Gaussian is also fitted in the lateral plane to allow 3D position determination.
- 25|** View the results using *showres*. Verify that the distribution is not too broad ( $\sigma = 10$  nm  $\rightarrow$  good,  $\sigma = 15$   $\rightarrow$  acceptable,  $\sigma = 20$   $\rightarrow$  microscope needs re-alignment). Also check that the estimated size does not vary across the field of view and that the estimated size is not more than around 30 nm larger than the nominal bead size. Save results (command *savefits\_rep*).
- 26|** If the above conditions are satisfied, the required correction factor for each bead is then stored in *umods*. Take the median of this value (less susceptible to potential clustering than the mean) and enter in the *umod* parameter field. This value represents the fraction of the illumination intensity that is not modulated.
- 27|** If multiple color channels were acquired, select the next channel and repeat Steps 22–26.
- 28|** Repeat Steps 21–27 for the remaining bead measurements, ensuring that the correct size is observed. This rules out the possibility of a false calibration owing to a preparation artifact, for example, air bubbles. The final bead measurements can then be used to verify that the measurement conditions were constant throughout the measurement series.

## Data analysis: biological measurements

- 29|** Open and evaluate biological acquisitions as per beads (Steps 21–28), using the previously determined *umod* value. Alternatively, open a few files by hand and determine a suitable value for the *ofind* threshold parameter. Note that this parameter is not the threshold itself, but rather used to guide an automated threshold procedure. Once set, it should perform reasonably well for all cells, provided the signal-to-background ratio and structure density are similar. It is probably better to err a little on the low side, as extra points can always be discarded after processing.
- 30|** Start batch mode processing and go for a coffee. Or start in the evening before going home, depending on data volume.
- 31|** Note that the evaluation of distance measurements is more complex, requiring a calibration of both focal plane curvature and wavefront tilt using the beads.

## Data analysis: position measurements

- 32|** Position measurements are automatically performed as part of the data analysis procedure detailed above and saved with the object sizes and other information. These position data are, however, not corrected for chromatic shift or wavefront tilt. The exact correction procedure depends on what form of calibration objects are available and how much accuracy is required. Calculate the wavefront tilt from a field of beads using the script *phasesurf* and determine the chromatic shift by comparing the apparent positions of calibration objects (e.g., Tetra-speck beads) in the different channels. Do the correction manually by subtracting the calculated shifts, either at the Matlab console or in Excel. For objects that are relatively close together, the wavefront tilt can be ignored and the chromatic shift can be eliminated by measuring distances to a common calibration object.

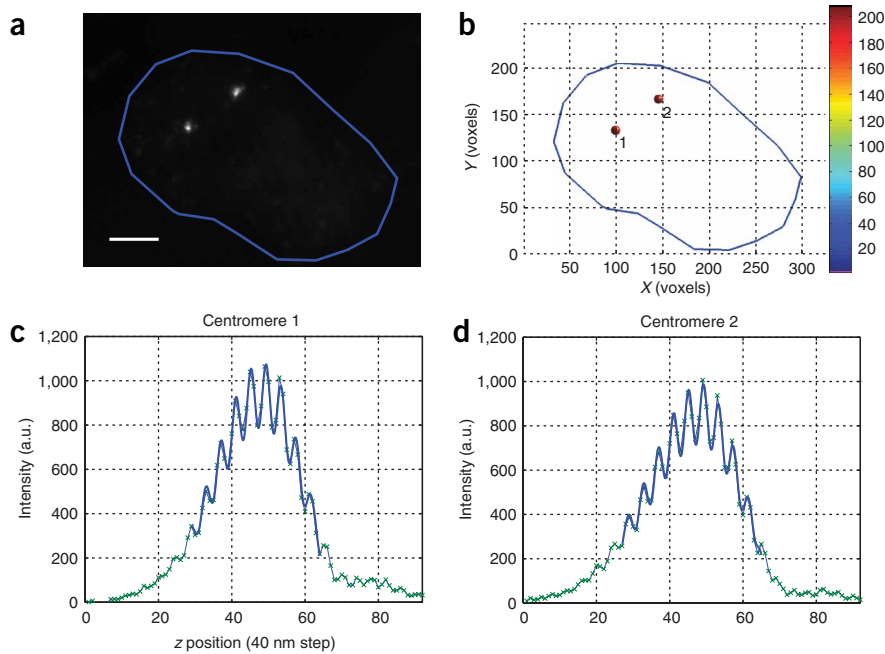
## Interpretation

- 33|** Compare results with model for biological object.

### ● TIMING

Biological preparation: depends on biological protocol  
 Steps 1–4, beads preparation: 10–20 min  
 Step 5, SMI warm-up: 1 h  
 Steps 6–12, initial bead measurements: 10–15 min

**Figure 2** | SMI measurements of fluorescence *in situ* hybridization-labeled centromere 8 regions in VH7 cells. (a) Raw image data (projection). Scale bar, 5  $\mu\text{m}$ . (b) Detected objects along with size estimate based on a spherical object form. Note that the assumption of spherical form for an extended centromere region is a poor assumption and the true sizes are almost certainly larger. (c,d) Axial profiles through the two centromeres, showing that a small amount of residual modulation is present, which can be attributed to the centromere not being entirely homogeneous.



Steps 14–17, cell measurements: depends on labeling intensity, cell density and cell thickness. Typically 2–3 min per cell and color channel. With good specimens, it is feasible to acquire 50–100 cells in an afternoon  
 Steps 21–28, analysis—calibration: approximately 5 min per bead acquisition (depends on the number of beads)  
 Steps 29 and 30, analysis—automated: depends on the number of loci; approximately 2 min per cell and color channel + 1 min per 100 loci

*Note:* The acquisition durations stated here include finding the cells and making all adjustments. They also assume a relatively weak signal and the desire to obtain the best photon statistics possible. Given appropriate labeling, it is possible to acquire a full 3D image stack in less than 10 s, making *in vivo* measurements feasible. A second SMI setup with water immersion and temperature control has been developed specifically for this purpose.

**? TROUBLESHOOTING**

**Step 15: Sparse cells**

If cells are sparsely spread and difficult to locate or one wishes to perform correlative microscopy, it is possible to relocate cells examined previously with, for example, a confocal microscope through use of a structured coverslip.

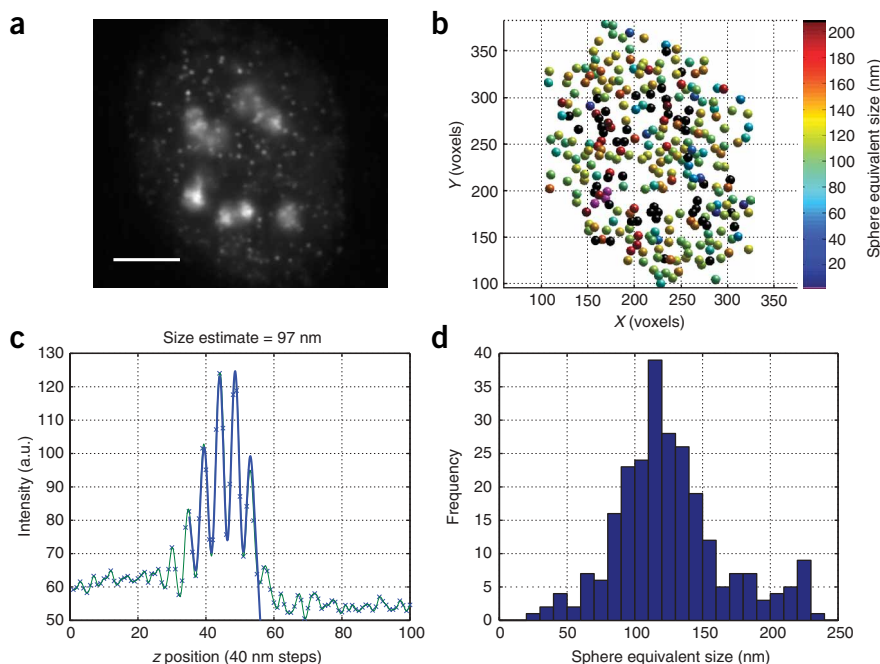


**Figure 3** | SMI measurements of the Ki-67 protein<sup>14</sup> (a proliferation marker protein) using a standard antibody protocol in VH7 cells. (a) Projection of raw image data. Scale bar, 5  $\mu\text{m}$ . (b) Automatically identified loci with size estimates. Whereas the larger structures evade sensible SMI size measurements (black/mauve spots), useful information can be gained from the smaller foci. (c) Fitted z profile of a typical locus. The crosses represent the raw data, the green line represents an interpolation of the raw data and the blue line represents the result of the fit to the raw data points over the central portion of the profile. To obtain the blue line, the fit function is evaluated at the locations of the data points and then interpolated to obtain a smooth curve for display (the tail at the right-hand end of the blue curve is the result of interpolating past the end of the last data point and has no consequence for the measurements). Note that the background level is estimated laterally from the area surrounding the focused object—the slight difference in background levels above and below the object is thus unimportant for the size estimation process. (d) Size distribution obtained from all successfully fitted loci.

**Steps 9 and 15: Focal plane/cells not found**

Finding the focal plane can be difficult if the fluorescent signal is very low. Either write down the position of the focus plane with other specimens, as the focal plane changes only by  $\sim 20 \mu\text{m}$  from sample to sample, or reduce the integration time to  $\sim 10 \text{ms}$  and use white light illumination to obtain images similar to phase contrast.

**Step 15: Relocation of cells at different microscopes**

Magnification is fixed in the SMI microscope, limiting the field of view to approximately  $50 \mu\text{m} \times 60 \mu\text{m}$ . Cells can be found more easily using a microscope with lower magnification. Use a micro-coordinator cover glass when preparing the samples. At the start of each measurement, record the 0-point of this coordinate grid and a prominent point on both axes of the coordinator before detection of the individual cell locations. By using a conversion algorithm, it is possible to relocate the positions of the cells using different microscope stages.

**ANTICIPATED RESULTS**

3D fluorescence images are produced, in which a characteristic modulation can be seen along the z axis (**Fig. 1b**). When prior information about the object form is available, or can be reasonably assumed, it is possible, through the use of an object model, to translate this modulation into a size estimate<sup>9,11</sup>. When the results from multiple cells are collected and categorized, size distributions are obtained, from which it should be possible to deduce structural differences in the measured objects. Example measurements from two different biological specimens are shown in **Figures 2 and 3**.

It is important to realize that SMI microscopy cannot deliver unambiguous size estimates for all objects. At the upper end of the size scale (size estimates  $> \sim 150 \text{nm}$ ), the errors induced by an assumption that it is a spherical object form can become significant. This is usually manifested in larger objects displaying a small residual modulation. **Figure 2** shows such a measurement in which centromere regions show a modulation depth of around 15%, which would correspond to a size of  $\sim 180 \text{nm}$  under the assumption of a spherical shape. The regions are, however, clearly larger than 250 nm, as some lateral structure is visible in the images. In such cases, it is best to regard the size estimate as a lower bound and, in general, size estimates on objects with a modulation depth of less than 20% should be approached with caution. The most likely reason for the residual modulation is an inhomogeneous fluorophore distribution within the object (see **Supplementary Manual**). In the case of smaller objects as shown in **Figure 3**, however, unambiguous size estimation is possible.

*Note: Supplementary information is available via the HTML version of this article.*

**ACKNOWLEDGMENTS** This work was sponsored by grants from the German Research Foundation (DFG CR 60/23-1+2) and by the European Commission (EU LSHG-CT-2003-503259 and MEIF-CT-2006-041827).

Published online at <http://www.natureprotocols.com>  
Reprints and permissions information is available online at <http://npg.nature.com/reprintsandpermissions>

1. Martin, S., Failla, A.V., Spöri, U., Cremer, C. & Pombo, A. Measuring the size of biological nanostructures with spatially modulated illumination microscopy. *Mol. Biol. Cell* **15**, 2449–2455 (2004).
2. Mathée, H. *et al.* Nanostructure of specific chromatin regions and nuclear complexes. *Histochem. Cell Biol.* **125**, 75–82 (2006).
3. Hell, S.W. & Wichmann, J. Breaking the diffraction resolution limit by stimulated emission: stimulated-emission-depletion fluorescence microscopy. *Opt. Lett.* **19**, 780–782 (1994).
4. Betzig, E. *et al.* Imaging intracellular fluorescent proteins at nanometer resolution. *Science* **313**, 1642–1645 (2006).
5. Hess, S.T., Girirajan, T.P. & Mason, M.D. Ultra-high resolution imaging by fluorescence photoactivation localization microscopy. *Biophys. J.* **91**, 4258–4272 (2006).
6. Rust, M.J., Bates, M. & Zhuang, X. Sub-diffraction-limit imaging by stochastic optical reconstruction microscopy (STORM). *Nat. Methods* **3**, 793–796 (2006).
7. Heintzmann, R., Jovin, T.M. & Cremer, C. Saturated patterned excitation microscopy—a concept for optical resolution improvement. *J. Opt. Soc. Am. A. Opt. Image Sci. Vis.* **19**, 1599–1609 (2002).
8. Gustafsson, M.G.L. Nonlinear structured-illumination microscopy: wide-field fluorescence imaging with theoretically unlimited resolution. *Proc. Natl. Acad. Sci. USA* **102**, 13081–13086 (2005).
9. Failla, A.V., Spoeri, U., Albrecht, B., Kroll, A. & Cremer, C. Nanosizing of fluorescent objects by spatially modulated illumination microscopy. *Appl. Opt.* **41**, 7275–7283 (2002).
10. Albrecht, B., Failla, A.V., Schweitzer, A. & Cremer, C. Spatially modulated illumination microscopy allows axial distance resolution in the nanometer range. *Appl. Opt.* **41**, 80–87 (2002).
11. Wagner, C., Hildenbrand, G., Spöri, U. & Cremer, C. Beyond nanosizing: an approach to shape analysis of fluorescent nanostructures by SMI-microscopy. *Optik* **117**, 26–32 (2006).
12. Egner, A. & Hell, S.W. Fluorescence microscopy with super-resolved optical sections. *Trends Cell Biol.* **15**, 207–215 (2005).
13. Jäckle, P. Temperaturstabilisierte Objekthalterung und chromatisches Korrekturlement zur Optimierung eines Zwei-Laser-Wellenfeld Mikroskops. Diploma Thesis, Universität Heidelberg, Heidelberg (1999).
14. Bridger, J.M., Kill, I.R. & Lichter, P. Association of pKi-67 with satellite DNA of the human genome in early G1 cells. *Chromosome Res.* **6**, 13–24 (1998).

